Published in final edited form as:
J Immunol. 2011 July 15; 187(2): 835–841. doi:10.4049/jimmunol.1100125.

Clonally-related CD8+ T cells responsible for rapid population of both d-NALT and lung after respiratory virus infection[1]

Sherri L. Surman[*], **Rajeev Rudraraju**[*], **David L. Woodland**[†], **Pradyot Dash**[‡], **Paul G. Thomas**[‡], and **Julia L. Hurwitz**[*,¶]

[*]Department of Infectious Diseases, St. Jude Children's Research Hospital, 262 Danny Thomas Place, Memphis, TN

[‡]Department of Immunology, St. Jude Children's Research Hospital, 262 Danny Thomas Place, Memphis, TN

[†]Trudeau Institute, 154 Algonquin Avenue, Saranac Lake, NY

[¶]Department of Microbiology, Immunology and Biochemistry, University of Tennessee, Memphis, TN

Abstract

The immune system has evolved to employ sophisticated mechanisms to recruit lymphocytes to sites of pathogen exposure. Trafficking pathways are precise. For example, lymphocytes which are primed by gut pathogens can in some cases be 'imprinted' with CCR9 membrane receptors, which can influence migration to the small intestine. Currently, little is known about T cell trafficking to the upper respiratory tract (URT) or the relationship between effectors that migrate to the diffuse nasal associated lymphoid tissues (d-NALT), the lower airways, and the lung. To determine whether a T cell primed by antigen from a respiratory pathogen is imprinted for exclusive trafficking to the upper or lower respiratory tract (LRT), or whether descendents from that cell have the capacity to migrate to both sites, we inoculated mice by the intranasal (I.N.) route with Sendai virus (SeV) and conducted single cell sequencing analyses of CD8+ T lymphocytes responsive to a K^b restricted immunodominant peptide, FAPGNYPAL (Tet+). Cells from the d-NALT, lung airways (bronchoalveolar lavage, BAL), lung and mediastinal lymph node (MLN) were examined 10 days after infection to determine TCR usage and clonal relationships. We discovered that: (i) Tet+ cells were heterogeneous, but preferentially utilized TCR elements TRAV6, TRAV16, and TRBD1, (ii) both N- and C- termini of Vα and Vβ TCR junctions frequently encompassed charged residues, perhaps facilitating TCR αβ pairing and interactions with a neutral target peptide, and (iii) a large fraction of the T cells in the d-NALT were clonal relatives of cells in the LRT.

INTRODUCTION

The immune system exhibits highly sophisticated lymphocyte trafficking patterns regulated by an array of adhesion molecules and chemokine receptors which 'imprint' lymphocytes at their site of first antigen exposure. A clear example of imprinting is illustrated by studies of gut-associated lymphoid tissues (GALT (1–3)). Induction of lymphocytes in the peyer's patches can preferentially commit these cells to GALT migration. The activated cells find

[1]This work was supported in part by NIH NIAID grants P01 AI054955, R01 AI088729, and R01 AI078819, NIH NCI grant P30 CA21765 and the American-Lebanese Syrian Associated Charities (ALSAC).

Corresponding Author: Julia L. Hurwitz, Department of Infectious Diseases, St. Jude Children's Research Hospital, 262 Danny Thomas Place, Memphis, TN 38105, Phone: 901-595-2464, FAX: 901-595-3099, julia.hurwitz@stjude.org.

their way to gut lamina propria via the thoracic duct and blood, directed in part by the membrane molecule α4:β7 which binds to MAdCAM-1 on endothelial cells. T cells marked with αe:β7 (CD103) can be rendered intra-epithelial cells due to their binding of e-cadherin on gut epithelium. Cells marked with CCR9 may bind CCL25 and preferentially reside in the small intestine while cells marked with CCR10 may bind CCL28 and preferentially reside elsewhere. Imprinting can enhance the efficiency of immune responses by directing activated lymphocytes to tissues where their specific antigen resides.

Surprisingly, despite a detailed understanding of T cell homing patterns in the gut, very little is known about cell homing to the upper respiratory tract (URT) in response to an intranasal (I.N.) virus infection. Improved analyses of T cell trafficking potentials in the respiratory tract are necessary to: (i) enhance our understanding of basic immune mechanisms and (ii) facilitate development of respiratory viral vaccines.

Once a virus enters the respiratory tract, it may persist in the upper airways for several days prior to migration to the LRT (4). This provides a window of opportunity for URT lymphocytes to inhibit infection before onset of LRT disease. A vaccine that induces robust and durable lymphocytes in nasal associated lymphoid tissues (NALT) is clearly much desired (5,6). There have been ongoing debates concerning the original activation sites of URT tissue-resident lymphocytes (7,8). When T cells are activated in URT and LRT lymph nodes, respectively, do they home predominantly to URT and LRT tissues (as depicted in Figure 1A)? Or can clonally-related descendents from a single activated T cell populate both URT and LRT after an I.N. virus exposure (as depicted in Figure 1B)?

Recent improvements in single cell sequencing (9,10) allow characterization of TCR α and β junctions in single cells and provide a means to define clonal-relatedness. Advanced tetramer technology further assists the focused study of CD8+ T cells with specificity for a model respiratory virus pathogen (11,12). By employing these sequencing and cell-marking tools, we now demonstrate that T cell trafficking can be flexible after a first exposure to a respiratory viral antigen. We show that T cell homing patterns support surveillance of both URT and LRT tissues by clonally-related cells.

MATERIALS AND METHODS

Animals and inoculations

Female C57BL/6J (B6; $H2^b$) mice were purchased from the Jackson Laboratory (Bar Harbor, ME). Animals were housed under specific pathogen-free conditions in a biosafety level 2+ containment area at the St. Jude animal facility, as specified by the Association for Assessment and Accreditation for Laboratory Animal Care (AAALAC) guidelines. Mice anesthetized with Avertin were infected I.N. with 250 plaque forming units (PFU) of SeV, Enders strain. Mice were approximately 2 months of age at the initiation of the immunization protocols.

Preparation of samples

Mice were exsanguinated upon treatment with avertin immediately prior to sacrifice. BAL were collected by inserting catheters into trachea and washing three times with 1 ml PBS. Wash samples were centrifuged to separate cellular material. To harvest d-NALT (13,14) animals were sacrificed and skin, lower jaws, soft palates (including the attached o-NALT), muscles, cheek bones and teeth were removed from the heads. O–NALT cells were not retained due to the difficulty of isolating these cells in the adult animal. Remaining snouts were cut into small pieces, after which cells were released by digestion with 4mg/ml collagenase in PBS at 37°C for 30 min. Cells were first washed with PBS and then suspended in PBS and layered onto a 40/75% discontinuous percoll gradient. After

centrifugation at 600 × g for 30 min, cells were collected from the gradient interface for assay. The cells were washed 2× in PBS and suspended in staining wash buffer (1% FBS in PBS). Lungs were suspended and similarly processed by collagenase digestion and purification on percoll gradients.

Single cell sorting

After removing the erythrocytes using RBC lysis buffer (8.3 g NH_4Cl, 1 g $KHCO_3$ and 1 ml of 0.1% Phenol Red in 1L of distilled water), the NALT, BAL, and Lung cells were treated with Fc block (Rat Anti-mouse CD16/CD32) separately and then stained using PE conjugated K^b $NP_{324–332}$ 12 tetramer at room temperature for 1 hr . Cells were resuspended in buffer(PBS + 2% BSA). Only the Tet+ cells were deposited as single cells into the wells of a 96-well PCR plate (Biorad) using a MoFlo flow cytometer (Cytomation, Fort Collins, CO, USA) fitted with a Cyclone single cell deposition unit. The last two columns of the plate were left blank for negative controls. After sorting, the plates were sealed using adhesive films and frozen at −80°C prior to RT-PCR. The IMGT database and software (www.imgt.org) facilitated the assignment of predicted V,D,J gene fragment usage.

Single cell RT-PCR, sequencing and cloning

The single cell sequencing reaction has been described previously (9,10). cDNA synthesis was performed with the iScript cDNA Synthesis Kit (Bio-Rad) as per manufacturer's instructions, with minor modifications. A 2.5 ul cDNA reaction was initiated in the individual wells in which single cells were deposited. The reaction consisted of 0.5 ul of 5X iScript reaction mix, 0.5 ul of iScript reverse transcriptase, 0.1% Triton X-100 (Sigma) and water. Incubations were at 25°C for 5 min, 42°C for 30 min, and 85°C for 5 min. Following RT a multiplex, nested PCR was performed with a Taq polymerase based PCR kit (Qiagen) to amplify the CDR3α and CDR3β transcripts from each cell in 25 ul reaction mixes containing 2.5 ul of cDNA (cDNA was not quantified prior to PCR). The first-round PCR was performed with 2.5 ul of 10X PCR buffer containing 15 mM $MgCl_2$, 0.5 ul of 10 mM dNTP, 0.75 units of Taq DNA polymerase, 0.5 ul of a oligonucleotide mixture of 23 TRAV forward primers, a single TRAC reverse primer, 19 TRBV forward primers and a single TRBC reverse primer (each 5 uM final concentration). A second round of PCR was then performed for CDR3α and CDR3β using product from the first PCR round as template and a similar primer mixture for the TRAV and TRBV internal primers. Primers have been described previously 9. The PCR conditions were 95 °C for 5 min, followed by 34 cycles of 95 °C for 20 sec, 56 °C for 20 sec, and 72 °C for 45 sec, with a final extension at 72 °C for 7 min. The PCR products were visualized on a 2% agarose gel and purified using a Wizard SV40 PCR purification kit (Promega). Sequencing was with TRAC or TRBC reverse primers for α and β PCR products, respectively, using a ABI Big Dye sequencer (Applied Biosystem) at the St. Jude Hartwell Center. The sequence data were analyzed using Chromas (Technelysium Pty Ltd) and MegAlign Software (DNASTAR Lasergene) and processed using a custom macro enabled Excel worksheet (9).

RESULTS

To identify patterns of T cell trafficking after SeV infection, we employed a C57BL/6 mouse model in which an immunodominant CD8+ T cell response had been defined. After an I.N. inoculation with SeV, the majority of CD8+ T cells responded to a K^b-restricted NP peptide 324–332 (FAPGNYPAL) and could be tracked by tetramer (Tet) reagent binding 12. Our experimental design involved the analysis of mice 10 days after an I.N. infection with 250 PFU SeV. Cells from d-NALT, lung and BAL were stained with the Tet reagent and individual cells were sorted into wells of microtiter plates. RNA was isolated and TCR Vα

and Vβ mRNAs were sequenced from individual wells. Three independent experiments were conducted (mouse 1, 2, 3).

Acutely responsive Tet+ T cells exhibit short, charged TCR CDR3 regions

A representative sampling of d-NALT cell TCRα V-J gene junctions (all captured from mouse 1) is shown in Table I. Identical sequences were often isolated from more than one cell as is indicated in Table I (the number of sequence repeats is shown in the second column). In the third column, Vα and Jα sequences are highlighted in red and green, respectively, demonstrating that junctions were of minimal size or absent among T cells acutely responsive to the SeV respiratory virus infection. In column 4, abbreviated junctional sequences are highlighted to indicate the positions of charged residues R, E, D, K, H (yellow), tyrosines (red), asparagines (blue) and phenylalanines (green). Charged residues often marked both 5' and 3' regions of the TCR V-Jα junctions.

In Table II is shown a sampling of d-NALT cell TCRβ sequences, isolated from the same mouse that was characterized in Table I. The frequencies of sequence isolation are shown in column two and the predicted V, D and J sequences are highlighted in red, blue and green, respectively, in column three. Again, CDR3 sizes were small. Also similar to the situation for TCR V-Jα junctions, V-D-Jβ junctions were often marked at the 5' and 3' ends by charged residues.

Preferential TCR gene usage in the acute response toward SeV

TCR α and β fragment usage is shown for Vα (column 2), Jα (column 3), Dβ (column 6) and Jβ (column 7) genes in Table III. Also shown are cases in which both α and β sequences were derived from a single well, as indicated by shared numbers in columns 4 and 8. In some cells, gene designations were not available due to ambiguities; Vβ gene designations were most often ambiguous and were not tabulated. Results revealed a heterogeneous T cell population in the d-NALT marked by high frequencies of TRAV6, TRAV16 and TRBD1. The TRBD1 gene was usually translated to amino acids DRG or a portion thereof, suggesting that the gene was read in its third reading frame (we note that due to similarities between TRBD1 and TRBD2, these fragment designations are not absolute). TRAV16 genes often encoded an arginine-glutamic acid (RE) sequence at the C terminus, while the DRBD1 gene often encoded an aspartic acid-arginine (DR) sequence when translated in its third reading frame, explaining in part the high frequency of charged residues in TCR junctions.

In Table IV is shown a compilation of d-NALT TCRα sequence data from the three different mice (mouse 1, mouse 2, mouse 3). As demonstrated, non-germline junctional sequences were consistently short, usually with no more than 1 or 2 amino acids between V, D or J fragments. In all three mice, there was frequent usage of TRAV16, TRAV6 and TRBD1. The RG amino acid sequence, typical of the third reading frame of TRBD1, was recognized in all but five d-NALT TCRα sequences.

Shared TCR junctions in d-NALT, lung and BAL

We next used the unique TCR junctions of individual T cells (15) as signature sequences to define the clonal relationships between cells from the URT and LRT. In Table VA, sequences that were shared by d-NALT, lung and BAL from mouse 1 were tabulated. The TCR α sequences were most informative as these were more plentiful than β sequences in our survey, but results were similar for both. The majority of all TCR α sequence junctions defined in this mouse were identified among cells in both the URT and LRT, suggesting that the cells in these two locations were usually clonally related. In some cases, an identical junctional sequence could be identified in all three tested tissues. In Table VB are shown

sequences that were identified in the BAL and lung, but not the d-NALT and in Table VC are shown sequences that were identified in only one of the three tissues.

In Table VI are shown sequences that were shared between URT and LRT in mouse 2 and mouse 3. In mouse 2, among 87 clones for which TCR α sequences could be defined, 50 exhibited sequences that were shared between URT and LRT samples. In mouse 3, among 59 clones for which TCR α sequences could be defined, 22 exhibited sequences that were shared between URT and LRT samples. In total, results revealed that ten days following infection with SeV, daughter T cells from common ancestor clones had populated both URT and LRT tissues.

An additional preliminary experiment was conducted to compare TCR sequences from d-NALT and the mediastinal lymph node (MLN), again to define clonal relationships. In this case, there were a number of clones identified from the two tissues that shared either TCR α or β junctional sequences (e.g. TCR α sequence REENTGNYKYVFGAGT, or TCR β sequences SGTGEVFFGKGTRLTV or SYYRGTNTEVFFGKGT). Clones were also identified from the two tissues that shared both TCR α and β sequences (REDNTGYQNFYFGKGT for TCR α and DRGYFAAGTR for TCR β) confirming their clonal relationship. Although the historical course of events associated with this outcome was not proven, a likely scenario is that precursor cells originated in the MLN and daughter cells trafficked to the d-NALT. These data again highlighted the natural potential of clonally related T cells to populate both the URT and LRT.

DISCUSSION

Clonally-related Tet+ T cells rapidly populate the URT and LRT after an acute respiratory virus infection

The current results clearly demonstrate that descendents from common precursor T cells have the capacity to populate both URT and LRT tissues within 10 days post-virus infection. The results supported the model in Figure 1B as daughters of activated T cells were multi-potent in terms of their trafficking potentials. This work addresses the debate regarding T cell migration potentials. T cells are not naturally imprinted to target one locale exclusively (URT versus LRT) in the respiratory tract.

Our data support a previous suggestion that T cell trafficking might be ‘promiscuous’. This notion was based on findings that responding T cells could be found in a number of different tissues (e.g. LRT, spleen, liver) after a virus infection, or upon adoptive transfer of memory cells into a naïve mouse (16). We confirm the suggestion by defining the clonal relationships associated with T cell migration. In our study, particular attention was paid to the URT as cells in this locale are best positioned to combat virus at its site of entry. Data in the current report further show that: (i) the trafficking destinations of clonally related cells include the d-NALT, BAL and lungs, (ii) the infiltration of URT and LRT tissues with clonally-related cells occurs as early as 10 days after an acute respiratory virus infection, and (iii) the rapid trafficking of clonally-related cells to URT and LRT tissues is a natural event which cannot be attributed to adoptive transfer manipulations.

Even though cells have the potential to traffic to both URT and LRT tissues, might they be influenced to populate one location preferentially (e.g. by administration of a vaccine that replicates predominantly in the URT)? It is of interest that the licensed cold-adapted influenza virus vaccine which grows predominantly in the URT associates with wheezing in some vaccinees (17). This consequence suggests that despite the cold-adapted nature of the vaccine, sufficient virus or viral antigen enters the LRT to recruit immune effectors. Ely et. al. have further demonstrated that activated T cells can infiltrate the LRT even when

inflammation is caused by an unrelated virus infection (18). We therefore propose that the induction of exclusive trafficking of T cells to the URT may be rare. Nonetheless, the fact that T cells resident in URT and LRT tissues differ in phenotype (6) suggests that biases in trafficking might be manipulated. Comprehensive studies are now warranted to further identify the membrane markers and trafficking potentials that define T cell homing and surveillance of the respiratory tract.

Skewed TCR usage among SeV-responsive cells

Our sequencing study revealed that the TCR usage among SeV-responsive cells was not random (TRAV 6/16 and TRBD1 gene fragments were frequently used), and that both α and β junctions were straddled by charged residues. This work expands upon a much smaller study conducted by Cole et. al. using hybridoma technology, in which arginine rich junctions of immunodominant $CD8^+$ T cells were noted (19). Possibly, arginines and the other charged residues identified in the current report assisted the binding of α and β chains to each other, after which a relatively neutral heterodimer associated with its neutral target peptide, FAPGNYPAL. The Vα sequence usage in the current study was much more heavily skewed compared to previously tested hybridomas. This is perhaps because cells in the current study were sorted based on binding to the FAPGNYPAL $–K^b$ tetramer, a technique which may have selected for a T cell sub-population with relatively high affinity for target peptide.

As stated above, there were a number of wells from which TCR α and β junctions could each be defined (Table 3, columns 4 and 8). When cells were defined as being clonally related based on one sequence (TCRα or TCRβ) and when the paired sequence (TCRβ or TCRα) could also be identified in that cell, the second sequence was usually also shared. However, there was an instance in which this was not the case. As shown in Table III, there were two cells that carried the TCRβ junction YFCASGGRGNQDTQYFGPGTR, yet expressed different α genes. These results might indicate that the two cells were derived from a common precursor with a rearranged β gene. After division, daughters may have rearranged and/or expressed different TCRα genes. This interpretation is consistent with the findings that TCR gene rearrangements often affect both chromosomes in a developing T cell and can be successive (20–24). Alteration of TCR gene usage among daughter cells may be due to differential transcription or translation of rearranged genes and/or by secondary rearrangements which occur either intrathymically or extrathymically (9,21,22,24–27). As one additional explanation, it is possible that on rare occasions, a shared junction in our study was not indicative of clonal relatedness, but was due to antigen selection of cells that coincidentally expressed identical TCR genes. In support of the latter argument, we found that upon review of hundreds of TCRα sequences from three different mice, there were three junctional sequences that appeared in more than one animal. Of note, shared junctional sequences were very rare when TCR sequences were compared among naïve mice (28).

SeV, an attractive vaccine vector for the respiratory viruses

The results in this report expand upon our understanding of the rapid lymphocyte responses to I.N. SeV. Indeed, heterogeneous CD8+ T cell populations, now known to derive from common precursors, are stationed in both the URT and LRT within days following a single I.N. inoculation. Respiratory tissues are populated by both T cells and plasma cells which persist for the lifetime of the animal 5. The capacity to induce long-lived B and T lymphocyte populations is an impressive feature of replication competent vaccines (29–31). Because SeV is a natural pathogen of mice and not humans (32), and because of its impressive similarities with the human parainfluenza virus type 1, the virus represents an attractive Jennerian vaccine candidate for croup (33–36). Additionally, SeV can be

manipulated by reverse genetics to express foreign genes (e.g. RSV F (37–39)) and to serve as a vaccine against several serious respiratory pathogens of children.

Acknowledgments

We thank Mark Sangster for useful discussions.

REFERENCES

1. Mora JR, Von Andrian UH. Differentiation and homing of IgA-secreting cells. Mucosal. Immunol. 2008; 1:96. [PubMed: 19079167]
2. Mora JR, Von Andrian UH. Role of retinoic acid in the imprinting of gut-homing IgA-secreting cells. Semin. Immunol. 2009; 21:28. [PubMed: 18804386]
3. Mora JR, Bono MR, Manjunath N, Weninger W, Cavanagh LL, Rosemblatt M, Von Andrian UH. Selective imprinting of gut-homing T cells by Peyer's patch dendritic cells. Nature. 2003; 424:88. [PubMed: 12840763]
4. Collins, PL.; Crowe, JE. Respiratory syncytial virus and metapneumovirus. In: Knipe, DM.; Howley, PM.; Griffin, DE.; Lamb, RA.; Martin, MA.; Roizman, B.; Straus, SE., editors. Fields Virology. Philadelphia, PA: Lippincott Williams&Wilkins; 2007. p. 1601
5. Sealy R, Jones BG, Surman SL, Hurwitz JL. Robust IgA and IgG-producing antibody forming cells in the diffuse-NALT and lungs of Sendai virus-vaccinated cotton rats associate with rapid protection against human parainfluenza virus-type 1. Vaccine. 2010; 28:6749. [PubMed: 20682364]
6. Rudraraju R, Surman S, Jones B, Sealy R, Woodland DL, Hurwitz JL. Phenotypes and functions of persistent Sendai virus-induced antibody forming cells and CD8+ T cells in diffuse nasal-associated lymphoid tissue typify lymphocyte responses of the gut. Virology. 2011; 410:429. [PubMed: 21227475]
7. Sabirov A, Metzger DW. Intranasal vaccination of infant mice induces protective immunity in the absence of nasal-associated lymphoid tissue. Vaccine. 2008; 26:1566. [PubMed: 18281130]
8. Kiyono H, Fukuyama. S. NALT versus Peyer's patch-mediated mucosal immunity. Nat. Rev. Immunol. 2004; 4:699. [PubMed: 15343369]
9. Dash P, McClaren JL, Oguin TH III, Rothwell W, Todd B, Morris MY, Becksfort J, Reynolds C, Brown SA, Doherty PC, Thomas PG. Paired analysis of TCRalpha and TCRbeta chains at the single-cell level in mice. J. Clin. Invest. 2010
10. Kedzierska K, Turner SJ, Doherty PC. Conserved T cell receptor usage in primary and recall responses to an immunodominant influenza virus nucleoprotein epitope 30. Proc. Natl. Acad. Sci. U. S. A. 2004; 101:4942. [PubMed: 15037737]
11. Klenerman P, Cerundolo V, Dunbar PR. Tracking T cells with tetramers: new tales from new tools. Nature Rev. Immunol. 2002; 2:263. [PubMed: 12001997]
12. Hogan RJ, Usherwood EJ, Zhong W, Roberts AA, Dutton RW, Harmsen AG, Woodland DL. Activated antigen-specific CD8+ T cells persist in the lungs following recovery from respiratory virus infections. J. Immunol. 2001; 166:1813. [PubMed: 11160228]
13. Davis SS. Nasal vaccines. Adv. Drug Deliv. Rev. 2001; 51:21. [PubMed: 11516777]
14. Asanuma H, Thompson AH, Iwasaki T, Sato Y, Inaba Y, Aizawa C, Kurata T, Tamura S. Isolation and characterization of mouse nasal-associated lymphoid tissue. J. Immunol. Methods. 1997; 202:123. [PubMed: 9107301]
15. Davis MM, Bjorkman PJ. T-cell antigen receptor genes and T-cell recognition. Nature. 1988; 334:395. [PubMed: 3043226]
16. Masopust D, Vezys V, Usherwood EJ, Cauley LS, Olson S, Marzo AL, Ward RL, Woodland DL, Lefrancois. L. Activated primary and memory CD8 T cells migrate to nonlymphoid tissues regardless of site of activation or tissue of origin. J. Immunol. 2004; 172:4875. [PubMed: 15067066]
17. Belshe RB, Edwards KM, Vesikari T, Black SV, Walker RE, Hultquist M, Kemble G, Connor EM. Live attenuated versus inactivated influenza vaccine in infants and young children. N. Engl. J. Med. 2007; 356:685. [PubMed: 17301299]

18. Ely KH, Cauley LS, Roberts AD, Brennan JW, Cookenham T, Woodland DL. Nonspecific recruitment of memory CD8+ T cells to the lung airways during respiratory virus infections. J. Immunol. 2003; 170:1423. [PubMed: 12538703]
19. Cole GA, Hogg TL, Woodland DL. The MHC class I-restricted T cell response to Sendai virus infection in C57BL/6 mice: a single immunodominant epitope elicits an extremely diverse repertoire of T cells. Int. Immunol. 1994; 6:1767. [PubMed: 7865469]
20. Hurwitz JL, Samaridis J, Pelkonen J. Immature and advanced patterns of T-cell receptor gene rearrangement among lymphocytes in splenic culture. J. Immunol. 1989; 142:2533. [PubMed: 2784465]
21. Thompson SD, Manzo AR, Pelkonen J, Larché M, Hurwitz JL. Developmental T-cell receptor gene rearrangements:Relatedness of the αβ and τδ T-cell precursor. Eur. J. Immunol. 1991; 21:1939. [PubMed: 1831133]
22. Thompson SD, Pelkonen J, Hurwitz JL. First T cell receptor α gene rearrangements during T cell ontogeny skew to the 5' region of the Jα locus. J. Immunol. 1990; 145:2347. [PubMed: 2168921]
23. Takeshita S, Toda M, Yamagishi H. Excision products of the T cell receptor gene support a progressive rearrangement model of the αδ locus. EMBO J. 1989; 8:3261. [PubMed: 2583098]
24. Hale JS, Wubeshet M, Fink PJ. TCR revision generates functional CD4+ T cells. J. Immunol. 2010; 185:6528. [PubMed: 20971922]
25. Thompson SD, Larche M, Manzo AR, Hurwitz JL. Diversity of T-cell receptor alpha gene transcripts in the newborn and adult periphery. Immunogenet. 1992; 36:95.
26. Cooper CJ, Orr MT, McMahan CJ, Fink PJ. T cell receptor revision does not solely target recent thymic emigrants. J. Immunol. 2003; 171:226. [PubMed: 12817002]
27. Serra P, Amrani A, Han B, Yamanouchi J, Thiessen SJ, Santamaria P. RAG-dependent peripheral T cell receptor diversification in CD8+ T lymphocytes. Proc. Natl. Acad. Sci. U. S. A. 2002; 99:15566. [PubMed: 12432095]
28. La Gruta NL, Rothwell WT, Cukalac T, Swan NG, Valkenburg SA, Kedzierska K, Thomas PG, Doherty PC, Turner SJ. Primary CTL response magnitude in mice is determined by the extent of naive T cell recruitment and subsequent clonal expansion. J. Clin. Invest. 2010; 120:1885. [PubMed: 20440073]
29. Crotty S, Felgner P, Davies H, Glidewell J, Villarreal L, Ahmed R. Cutting edge: long-term B cell memory in humans after smallpox vaccination. J Immunol. 2003; 171:4969. [PubMed: 14607890]
30. Amanna IJ, Slifka MK, Crotty S. Immunity and immunological memory following smallpox vaccination. Immunol. Rev. 2006; 211:320. [PubMed: 16824139]
31. Hyland L, Sangster M, Sealy R, Coleclough C. Respiratory virus infection of mice provokes a permanent humoral immune response. J. Virol. 1994; 68:6083. [PubMed: 8057487]
32. Karron, RA.; Collins, PL. Parainfluenza Viruses. In: Knipe, DM.; Howley, PM.; Griffin, DE.; Lamb, RA.; Martin, MA.; Roizman, B.; Straus, SE., editors. Fields Virology. Lippincott Williams and Wilkins; 2007. p. 1497
33. Hurwitz JL, Soike KF, Sangster MY, Portner A, Sealy RE, Dawson DH, Coleclough C. Intranasal Sendai virus vaccine protects African green monkeys from infection with human parainfluenza virus-type one. Vaccine. 1997; 15:533. [PubMed: 9160521]
34. Slobod KS, Shenep JL, Lujan-Zilbermann J, Allison K, Brown B, Scroggs RA, Portner A, Coleclough C, Hurwitz JL. Safety and immunogenicity of intranasal murine parainfluenza virus type 1 (Sendai virus) in healthy human adults. Vaccine. 2004; 22:3182. [PubMed: 15297072]
35. Lyn D, Gill DS, Scroggs RA, Portner A. The nucleoproteins of human parainfluenza virus type 1 and Sendai virus share amino acid sequences and antigenic and structural determinants. J. Gen. Vir. 1991; 72:983.
36. Sangster M, Smith FS, Coleclough C, Hurwitz JL. Human parainfluenza virus-type 1 immunization of infant mice protects from subsequent Sendai virus infection. Virology. 1995; 212:13. [PubMed: 7676623]
37. Jones B, Zhan X, Mishin V, Slobod KS, Surman S, Russell CJ, Portner A, Hurwitz JL. Human PIV-2 recombinant Sendai virus (rSeV) elicits durable immunity and combines with two additional rSeVs to protect against hPIV-1, hPIV-2, hPIV-3, and RSV. Vaccine. 2009; 27:1848. [PubMed: 19200447]

38. Zhan X, Slobod KS, Krishnamurthy S, Luque LE, Takimoto T, Jones B, Surman S, Russell CJ, Portner A, Hurwitz JL. Sendai virus recombinant vaccine expressing hPIV-3 HN or F elicits protective immunity and combines with a second recombinant to prevent hPIV-1, hPIV-3 and RSV infections. Vaccine. 2008; 26:3480. [PubMed: 18499307]

39. Zhan X, Hurwitz JL, Krishnamurthy S, Takimoto T, Boyd K, Scroggs RA, Surman S, Portner A, Slobod KS. Respiratory syncytial virus (RSV) fusion protein expressed by recombinant Sendai virus elicits B-cell and T-cell responses in cotton rats and confers protection against RSV subtypes A and B. Vaccine. 2007; 25:8782. [PubMed: 18037543]

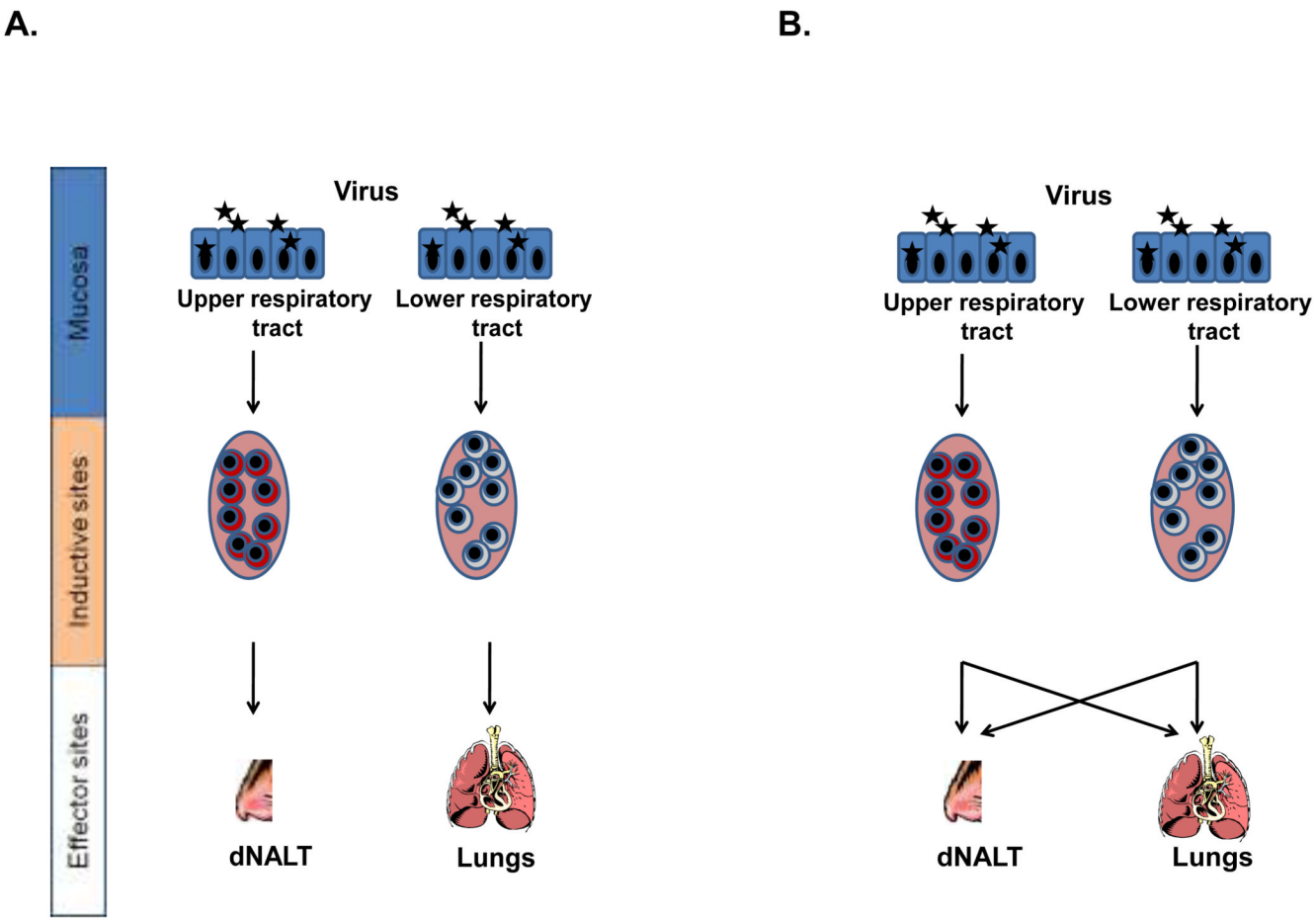

Figure 1. Models of homing patterns in the respiratory tract

The cartoon describes two hypotheses concerning the trafficking of activated T cells within the respiratory tract. Figure 1a suggests a commitment of cells primed in the URT to home exclusively to the URT (and cells primed in the LRT to home exclusively to the LRT) while figure 1B suggests that the site of priming will not restrict homing potentials to URT and LRT tissues.

Table I

Charged amino acid residues at N and C termini of TCRα junctions

Sequence	[a]replicate isolations	[b]V-Jα Sequences	[c]TCRα junctions
1	8	CAMREDNYAQGLTFGLGTR	REDNYAQGLTFGLGTR
2	6	CALGGANTNKVVFGTGTRL	GGANTNKVVFGTGTRL
3	4	CAMRDTNAYKVIFGKGTHLH	RDTNAYKVIFGKGTHLH
4	3	CAMREGNMGYKLTFGTGTS	REGNMGYKLTFGTGTS
5	3	CAMREGDYANKMIFGLGTI	REGDYANKMIFGLGTI
6	3	CATDDSGGYKVVFGSGTRL	DDSGGYKVVFGSGTRL
7	2	CAMREDNTGYQNFYFGKGT	REDNTGYQNFYFGKGT
8	1	CAMREGDDSGYNKLTFGKG	REGDDSGYNKLTFGKG
9	1	CALGEENSNNRIFFGDGTQ	GEENSNNRIFFGDGTQ
10	1	CAMREHMATGGNNKLTFGQ	REHMATGGNNKLTFGQ
11	1	CAMREANMGYKLTFGTGTS	REANMGYKLTFGTGTS
12	1	CAAMGYSNNRLTLGKGTQV	MGYSNNRLTLGKGTQV
13	1	REDNTNKVVFGTGTRL	REDNTNKVVFGTGTRL
14	1	CAMREVNTGNYKYVFGAGT	REVNTGNYKYVFGAGT
15	1	CAMREGDSAGNKLTFG	REGDSAGNKLTFG
16	1	CAIDTNAYKVIFGKGTH	DTNAYKVIFGKGTH
17	1	CAARVAGSGGKLTLGAGTR	RVAGSGGKLTLGAGTR
18	1	CAALDTNAYKVIFGKGTHL	LDTNAYKVIFGKGTHL
19	1	CAMREDENMGYKLTFGTGT	REDENMGYKLTFGTGT
20	1	CAVKGGNYKPTFGKGTSLV	KGGNYKPTFGKGTSLV
21	1	CAMREDTNTGKLTFGDGTV	REDTNTGKLTFGDGTV
22	1	CAILLDYANKMIFGLGTIL	LLDYANKMIFGLGTIL
23	1	CALGDLNSGSWQLIFGSGT	GDLNSGSWQLIFGSGT
24	1	CALVRTGGYKVVFGSGTRL	VRTGGYKVVFGSGTRL
25	1	CAAGGDNRIFFGDGTQLVV	GGDNRIFFGDGTQLVV

TCR Vα sequences are listed for one representative experiment (mouse 1) among 3 independent experiments.

[a]The number of clones that shared each sequence in the d-NALT.

[b]Predicted positions of Vα and Jα (red and green).

[c]positions of charged residues R,E,D,K,H (yellow), tyrosines (red), asparagines (blue) and phenylalanines (green).

Table II

Charged amino acid residues at N and C termini of TCRβ junctions

Sequence	[a]replicate isolations	[b]V-D-Jβ Sequences	[c]TCRβ junctions
1	4	YFCASRDRGSQNTLYFGAGTR	RDRGSQNTLYFGAGTR
2	4	YFCASGERGHTNERLFFGHGT	GERGHTNERLFFGHGT
3	3	YFCASSDARGTNERLFFGHGT	SDARGTNERLFFGHGT
4	2	YFCASSLTGRGANTEVFFGKG	SLTGRGANTEVFFGKG
5	2	SSADRGRRAETLYFGSG	SADRGRRAETLYFGSG
6	2	YFCASGGRGNQDTQYFGPGTR	GGRGNQDTQYFGPGTR
7	1	YLCASSFRGALDTQYFGPGTR	SFRGALDTQYFGPGTR
8	1	YFCASSPRGAETLYFGSGTRL	SPRGAETLYFGSGTRL
9	1	YLCASSLDRGSGNTLYFGEGS	SLDRGSGNTLYFGEGS
10	1	YLCASSRDRSNSDYTFGSGTR	SRDRSNSDYTFGSGTR
11	1	YLCASSFGRGTDTEVFFGKGT	SFGRGTDTEVFFGKGT
12	1	YLCASRPRGGQDTQYFGPGTR	RPRGGQDTQYFGPGTR
13	1	YLCASRDRGNSDYTFGSGTRL	RDRGNSDYTFGSGTRL
14	1	FLCASSARTNNNQAPLFGEGT	SARTNNNQAPLFGEGT
15	1	YFCASSDRGAQNTLYFGAGTR	SDRGAQNTLYFGAGTR
16	1	YFCASGDRGGDYAEQFFGPG	GDRGGDYAEQFFGPG
17	1	YFCASSRDRGGTEVFFGKGTR	SRDRGGTEVFFGKGTR
18	1	YFCASSDRGNQDTQYFGPGTR	SDRGNQDTQYFGPGTR

TCR Vβ sequences are listed for one representative experiment among 3 independent experiments.

[a]The number of clones that shared each sequence in the d-NALT.

[b]Predicted positions of Vβ, Dβ and Jβ (red, blue and green).

[c]positions of charged residues R,E,D,K,H (yellow), tyrosines (red), asparagines (blue) and phenylalanines (green).

Table III

TCR gene fragment usage

V-J Alpha Sequences	^{a}TRAV	^{a}TRAJ	^{b}TCR αβ sharing	V-D-J Beta Sequences	^{a}TRBD	^{a}TRBJ	^{b}TCR αβ sharing
CAMREDNYAQGLTFGLGTR	16	26	1	YFCASRDRGSQNTLYFGAGTR	1	2-4	4
CALGGANTNKVVFGTGTRL	6	34	4	YFCASGERGHTNERLFFGHGT	1	1-4	14
CAMRDTNAYKVIFGKGTHLH	16	30	7	YFCASSDARGTNERLFFGHGT	1	1-4	1
CAMREGNMGYKLTFGTGTS	16	9	2	YFCASSLTGRGANTEVFFGKG	1	1-1	2
CAMREGDYANKMIFGLGTI	16	47	3	SSADRGRRAETLYFGSG	1	2-3	6
CATDDSGGYKVVFGSGTRL	8	12		YFCASGGRGNQDTQYFGPGTR	1	2-5	11,13
CAMREDNTGYQNFYFGKGT	16	49	10	YLCASSFRGALDTQYFGPGTR	1	2-5	3
CAMREGDDSGYNKLTFGKG	16	11	11	YFCASSPRGAETLYFGSGTRL	1	2-3	5
CALGEENSNNRIFFGDGTQ	6	31	14	YLCASSLDRGSGNTLYFGEGS	1	1-3	1
CAMREHMATGGNNKLTFGQ	16	56	15	YLCASSRDRSNSDYTFGSGTR	1	1-2	7
CAMREANMGYKLTFGTGTS	16	9		YLCASSFGRGTDTEVFFGKGT	1	1-1	8
CAAMGYSNNRLTLGKGTQV	ND	7		YLCASRPRGGQDTQYFGPGTR	1	2-5	9
REDNTNKVVFGTGTRL	16	34	8	YLCASRDRGNSDYTFGSGTRL	1	1-2	
CAMREVNTGNYKYVFGAGT	16	40		FLCASSARTNNNQAPLFGEGT	1	1-5	7
CAMREGDSAGNKLTFG	16	17		YFCASSDRGAQNTLYFGAGTR	1	2-4	
CAIDTNAYKVIFGKGTH	13	30	9	YFCASGDRGGDYAEQFFGPG	1	2-1	10
CAARVAGSGGKLTLGAGTR	ND	44	5	YFCASSRDRGGTEVFFGKGTR	1	1-1	12
CAALDTNAYKVIFGKGTHL	ND	30	6	YFCASSDRGNQDTQYFGPGTR	1	2-5	14
CAMREDENMGYKLTFGTGT	16	9					
CAVKGGNYKPTFGKGTSLV	ND	6					
CAMREDTNTGKLTFGDGTV	16	27					

V-J Alpha Sequences	^{a}TRAV	^{a}TRAJ	^{b}TCR αβ sharing	V-D-J Beta Sequences	^{a}TRBD	^{a}TRBJ	^{b}TCR αβ sharing
CAILLDYANKMIFGLGTIL	ND	47					
CALGDLNSGSWQLIFGSGT	6	22	12				
CALVRTGGYKVVFGSGTRL	6	12	13				
CAAGGDNRIFFGDGTQLVV	19	31					

^{a}Predicted gene usage; TRAV gene designations (ND, not determined). Many TRBV gene designations were ambiguous and are not shown. TRBD gene predictions are not definitive due to the close similarities between TRBD1 and TRBD2.

^{b}Shared numbers indicate identification of TCR α and β sequences in the same cell.

Table IV

Frequency of sequence characteristics among single cells

TCRα	***Incidence of predicted V-J non-germline junctional sequence size**					**#TRAV16 (#TRAV6)**	**Total # unique amino acid sequences**
	0 aa	**1 aa**	**2 aa**	**3 aa**	**4 aa**		
Mouse 1	3	9	11	2	0	13 (4)	25
Mouse 2	2	9	4	1	0	11 (3)	16
Mouse 3	4	6	7	3	0	11 (1)	20
TCRβ	*Incidence of maximal predicted V-D or D-J non-germline junctional sequence size					# sequences with amino acids RG in TRBD position	Total # unique amino acid sequences
	0 aa	1 aa	2 aa	3 aa	4 aa		
Mouse 1	2	8	8	0	0	16	18
Mouse 2	3	9	4	0	0	14	16
Mouse 3	0	3	5	0	1	8	9

* A composite of data is shown for three individual mice. The number of sequences with various sizes of predicted non-germline amino acids between V-J α, V-Dβ, or D-Jβ is shown. Also shown are the numbers of sequences with TRAV16 or TRAV6 usage, or with the amino acids RG in the position of TRBD.

Table V

Shared junctional sequences in the d-NALT, lung and BAL of Mouse 1

d-NALT V alpha	Lung V Alpha	BAL V Alpha
A. MOUSE 1: SHARED SEQUENCES BETWEEN URT AND LRT (number of single cells per tissue sharing sequence)		
REDNYAQGLTFGLGTR (8)	REDNYAQGLTFGLGTR (4)	REDNYAQGLTFGLGTR (6)
GGANTNKVVFGTGTRL (6)	GGANTNKVVFGTGTRL (2)	GGANTNKVVFGTGTRL (2)
RDTNAYKVIFGKGTHL (4)	RDTNAYKVIFGKGTHL (1)	RDTNAYKVIFGKGTHL (5)
REGNMGYKLTFGTGTS (3)	REGNMGYKLTFGTGTS (2)	REGNMGYKLTFGTGTS (1)
REGDYANKMIFGLGTI (3)	REGDYANKMIFGLGTI (2)	REGDYANKMIFGLGTI (4)
REDNTGYQNFYFGKGT (2)	REDNTGYQNFYFGKGT (1)	REDNTGYQNFYFGKGT (2)
REGDDSGYNKLTFGKG (1)	REGDDSGYNKLTFGKG (2)	REGDDSGYNKLTFGKG (1)
GEENSNNRIFFGDGTQ (1)	GEENSNNRIFFGDGTQ (1)	-
REHMATGGNNKLTFGQ (1)	REHMATGGNNKLTFGQ (1)	-
AALDTNAYKVIFGKGTHL (1)	AALDTNAYKVIFGKGTHL (1)	
REANMGYKLTFGTGTS (1)	-	REANMGYKLTFGTGTS (1)
MGYSNNRLTLGKGTQV (1)	-	MGYSNNRLTLGKGTQV (1)
REDNTNKVVFGTGTRL (1)	-	REDNTNKVVFGTGTRL (2)
B. MOUSE 1: SHARED SEQUENCES BETWEEN LUNG AND BAL		
	REDMGYKLTFGTGTSL (1)	REDMGYKLTFGTGTSL (1)
C. MOUSE 1: UNSHARED SEQUENCES		
DDSGGYKVVFGSGTRL (3)		
REVNTGNYKYVFGAGT (1)		
REGDSAGNKLTFG (1)		SDYNVGDNSKLIWGLG (1)
DTNAYKVIFGKGTHLH (1)		DAQTQVVGQLTFGRGT (1)
RVAGSGGKLTLGAGTR (1)	SDTNAYKVIFGKGTHL (1)	EGGRALIFGTGTTVSV (1)
REDENMGYKLTFGTGT (1)	REGRATGGNNKLTFGQ (1)	ETNYNVLYFGSGTKLT (1)
KGGNYKPTFGKGTSLV (1)	GDTNAYKVIFGKG (1)	GDLGVATGGNNKLTFG (1)
REDTNTGKLTFGDGTV (1)	-	VRTGGYKVVFGSGTRL (1)
LLDYANKMIFGLGTIL (1)	-	NGGDTNAYKVIFGKGTHL (1)
GDLNSGSWQLIFGSGT (1)	-	REGGTNAYKVIFGKGT (3)
VRTGGYKVVFGSGTRL (1)	-	-
GGDNRIFFGDGTQLVV (1)	-	-

Legend: TCRα sequences from d-NALT, BAL and lung are listed to demonstrate sharing of precise TCRα junctions.

Table VI

Shared junctional sequences in the d-NALT, lung and BAL in Mouse 2 and Mouse 3

d-NALT V alpha	Lung V Alpha	BAL V Alpha
A. Mouse 2: SHARED SEQUENCES BETWEEN URT AND LRT (number of single cells per tissue sharing sequence)		
REDNYAQGLTFGLGTR (2)	REDNYAQGLTFGLGTR (3)	REDNYAQGLTFGLGTR (3)
REDNTGNYKYVFGAGT (2)	REDNTGNYKYVFGAGT (1)	REDNTGNYKYVFGAGT (1)
REGDGTGSKLSFGKGA (2)	REGDGTGSKLSFGKGA (1)	REGDGTGSKLSFGKGA (3)
GDPDNAGAKLTFGGGT (1)	GDPDNAGAKLTFGGGT (1)	GDPDNAGAKLTFGGGT (2)
GGSNTNKVVFGTGTRL (3)	GGSNTNKVVFGTGTRL (3)	
RDNNYAQGLTFGLGTR (3)	RDNNYAQGLTFGLGTR (2)	
REEYANKMIFGLGTIL (2)	REEYANKMIFGLGTIL (1)	
MRDTNAYKVIFGKGTHL (1)	MRDTNAYKVIFGKGTHL (4)	
REDNNNNAPRFGAGTK (1)	REDNNNNAPRFGAGTK (2)	
DPMDSNYQLIWGSGTK (1)	DPMDSNYQLIWGSGTK (1)	
REVDTNTGKLTFGDGT (1)	REVDTNTGKLTFGDGT (1)	
SIGTGNTGKLIFGLGT (1)	SIGTGNTGKLIFGLGT (1)	
B. MOUSE 3: SHARED SEQUENCES BETWEEN URT AND LRT (number of single cells per tissue sharing sequence)		
REIMDSNYQLIWGSGT (8)	REIMDSNYQLIWGSGT (3)	REIMDSNYQLIWGSGT (4)
REGDSNNRIFFGDGTQ (1)	REGDSNNRIFFGDGTQ (1)	
TDYSNNRLTLGKGTQVV (1)		TDYSNNRLTLGKGTQVV (1)
AGDTNAYKVIFGKGTHL (2)		AGDTNAYKVIFGKGTHL (1)

Legend: TCRα sequences from d-NALT, BAL and lung are listed to demonstrate sharing of precise TCRα junctions. In mouse 2, there were 87 clones for which TCR α sequences could be defined. Listed are the 50 sequences that were shared between URT and LRT samples. In mouse 3, there were 59 clones for which TCR α sequences could be defined. Listed are the 22 sequences that were shared between URT and LRT.